Deep Learning-Aided Projected Gradient Detector for Massive Overloaded MIMO Channels

Satoshi Takabe*†, Masayuki Imanishi*, Tadashi Wadayama*, and Kazunori Hayashi‡

*Nagoya Institute of Technology, Gokiso, Nagoya, Aichi 466-8555, Japan,
s_takabe@nitech.ac.jp, 29414024@stn.nitech.ac.jp, wadayama@nitech.ac.jp
†RIKEN Center for Advanced Intelligence Project, Nihonbashi, Chuo-ku, Tokyo 103-0027, Japan
‡Graduate School of Engineering, Osaka City University, Sugimoto, Sumiyoshi-ku, Osaka, 558-8585, Japan,
kazunori@eng.osaka-cu.ac.jp

Abstract—**The paper presents a deep learning-aided iterative detection algorithm for massive overloaded MIMO systems. Since the proposed algorithm is based on the projected gradient descent method with trainable parameters, it is named as trainable projected descent-detector (TPG-detector). The trainable internal parameters can be optimized with standard deep learning techniques such as back propagation and stochastic gradient descent algorithms. This approach referred to as data-driven tuning brings notable advantages of the proposed scheme such as fast convergence. The numerical experiments show that TPG-detector achieves comparable detection performance to those of the known algorithms for massive overloaded MIMO channels with lower computation cost.**

I. Introduction

Multiple input multiple output (MIMO) systems have attracted great interests because they potentially achieve high spectral efficiency in wireless communications. Recently, as a consequence of high growth of mobile data traffic, *massive* MIMO is regarded as a key technology in the 5th generation (5G) wireless network standard [1]. In massive MIMO systems, tens or hundreds of antennas are used in the transmitter and the receiver. This fact complicates the detection problem for MIMO channels because the computational complexity of a MIMO detector, in general, increases as the numbers of antennas grow. A practical massive MIMO detection algorithm should possess both low energy consumption and low computational complexity in addition to reasonable bit error rate (BER) performance.

In a down-link massive MIMO channel with mobile terminals, a transmitter in a base station can have many antennas but a mobile terminal cannot have such a number of receive antennas because of the restrictions on cost, space limitation, and power consumption. This scenario is known as the *overloaded* (or *underdetermined*) scenario. Development of an overloaded MIMO detector with computational efficiency and reasonable BER performance is a highly challenging problem because conventional naive MIMO decoders such as the minimum mean square error (MMSE) detector [2] exhibit poor BER performance for overloaded MIMO channels, and an optimal detection based on the exhaustive search is evidently computationally intractable.

Several search-based detection algorithms such as slab-sphere decoding [3] and enhanced reactive tabu search (ERTS) [4] have been proposed for overloaded MIMO channels. Though these schemes show excellent detection performance, they are computationally demanding, and it may prevent us from implementing them into a practical massive overloaded MIMO system. As a computationally efficient approach based on the ℓ_1-regularized minimization, Fadlallah et. al proposed a detector using a convex optimization solver [5]. Recently, Hayakawa and Hayashi [6] proposed an iterative detection algorithm with practical computational complexity called *iterative weighted sum-of-absolute value* (IW-SOAV) optimization (see also [7]). The algorithm is based on the SOAV optimization [8] for sparse discrete signal recovery. In addition, the algorithm includes a re-weighting process based on the log-likelihood ratio, which improves the detection performance. The IW-SOAV provides the state-of-the-art BER performance among overloaded MIMO detection algorithms with low computational complexity.

The use of deep neural networks has spread to numerous fields such as image recognition [9] with the progress of computational resources. It also gives a great impact on design of algorithms for wireless communications and signal processing [10], [11]. Gregor and LeCun first proposed the learned iterative shrinkage-thresholding algorithm (LISTA) [12], which exhibits better recovery performance than that of the original ISTA [13] for sparse signal recovery problems. Recently, the authors proposed the *trainable ISTA* (TISTA) [14] yielding significantly faster convergence than ISTA and LISTA.

TISTA includes several trainable internal parameters and these parameter are tuned with standard deep learning techniques such as back propagation and stochastic gradient descent (SGD) algorithms. From our research work on TISTA [14] and several additional experiments (an example will be presented in Section III), we encountered a phenomenon that the convergence to the minimum value is accelerated with appropriate parameter embedding for several numerical optimization algorithms such as the projected gradient descent method and the proximal gradient method. We call this phenomenon *data-driven acceleration* of convergence.

Most of known acceleration techniques for gradient descent

algorithms such as the momentum methods do not care about the statistical nature of the problems. On the other hand, the data-driven acceleration is obtained by learning the statistical nature of the problem, i.e., stochastic variations on the landscape of the objective functions. The internal parameters controlling the behavior of the algorithm are adjusted to match the typical objective function via training processes. The data-driven acceleration is especially advantageous in implementation of detection algorithms because it reduces the number of iterations without sacrificing the detection performance. This makes the algorithm faster and more power efficient.

The goal of this paper is to propose a novel detection algorithm for massive overloaded MIMO systems, which is called *Trainable Projected Gradient-Detector* (TPG-detector). The proposed algorithm is based on the projected gradient descent method with trainable parameters. We have confirmed that data-driven acceleration improves the detection performance and the convergence speed. Though deep learning architectures for massive MIMO systems were recently proposed as deep MIMO detectors (DMDs) in [15], [16], no deep learning-aided iterative detectors for massive *overloaded* MIMO channels have been proposed as far as the authors are aware of. Furthermore, an application of data-driven tuning to MIMO detectors has not yet been studied in the related literatures.

II. DATA-DRIVEN TUNING

We here introduce the concept of the *data-driven tuning of numerical optimization algorithms*, whose origin is the work by Gregor and LeCun [12]. For improving the performance of a numerical optimization algorithm, several trainable parameters can be embedded in the algorithm. By unfolding an iterative process of a numerical optimization algorithm, we have a multilayer signal-flow graph that is similar to a deep neural network. Since each component of the signal-flow graph is differentiable, these trainable parameters can be adjusted by standard deep learning techniques. The training data can be randomly generated according to a channel model.

Figure 1 (a) illustrates a signal-flow diagram of an iterative numerical optimization algorithm where Processes A, B, and C are processes whose input/output relationships are expressed with differentiable functions. By unfolding the signal-flow diagram, we obtain a signal-flow graph similar to a multilayer neural network (Fig. 1(b)).

Each process contains trainable parameters that are represented by the black circles in Fig. 1(b). The trainable parameters can control behavior of the processes A, B, and C. Appending a loss function, e.g., the squared loss function, at the end of the unfolded signal-flow graph, we are ready to feed randomly generated training data to the graph. We can apply back propagation and a SGD type parameter update (SGD, RMSprop, Adam, etc.) to optimize the parameters.

III. DATA-DRIVEN ACCELERATION

We now discuss a simple example of the data-driven acceleration in more detail. As a toy model closely related to
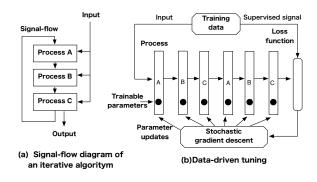

Fig. 1. (a) A signal-flow diagram of an iterative algorithm, (b) Data-driving tuning based on an unfolded signal-flow graph with a loss function

the MIMO channel, we consider a quadratic programming problem with binary variables.

Let us consider a simple quadratic optimization problem

$$\text{minimize } \frac{1}{2}\|Ax - y\|_2^2 \text{ subject to } x \in \{-1, +1\}^n, \quad (1)$$

where $A \in \mathbb{R}^{n \times n}$ is a given matrix and $\|\cdot\|_2$ represents the Euclidean norm. We assume that y is stochastically generated as $y = A\tilde{x} + w \in \mathbb{R}^n$ where $\tilde{x}$ is a vector randomly sampled from $\{-1, +1\}^n$ uniformly at random and $w \in \mathbb{R}^n$ consists of i.i.d. Gaussian random variables with zero mean and variance σ^2. The optimization problem is essentially same as the maximum likelihood estimation rule for the Gaussian linear vector channel.

Since solving this problem is known as an NP-hard problem in general, we need to solve the problem approximately. We here exploit a valiant of the projected gradient (PG) algorithm to solve (1) approximately. The PG algorithm can be described by the recursive formula:

$$r_t = s_t + \gamma A^T(y - As_t), \quad (2)$$
$$s_{t+1} = \tanh(\alpha r_t), \quad (3)$$

where $t = 1, \ldots, T$ and $\tanh(\cdot)$ is calculated element-wisely.

The PG algorithm consists of two computational steps for each iteration. In the gradient descent step (2), a search point moves to the opposite direction to the gradient of the objective function, i.e., $\nabla \frac{1}{2}\|Ax - y\|_2^2 = -A^T(y - Ax)$. The parameter γ controls the step size causing critical influence on the convergence behavior. In the projection step (3), *soft-projection* based on the hyperbolic tangent function is applied to the search point to obtain a new search point nearly rounded to binary values. Precisely speaking, the projection step is not the projection to the binary symbols $\{-1, +1\}$. This is because the true projection to discrete values results in insufficient convergence behavior in a minimization process. The parameter α controls the softness of the soft projection. Note that this type of nonlinear projection has been commonly used in several iterative multiuser detection algorithms such as the soft parallel interference canceller [17].

According to the data-driven tuning framework, we can embed trainable parameters into the PG algorithm. The trainable PG (TPG) algorithm is based on the recursion

$$r_t = s_t + \gamma_t A^T(y - As_t), \tag{4}$$

$$s_{t+1} = \tanh(\alpha r_t). \tag{5}$$

The trainable parameters $\{\gamma_t\}_{t=1}^T$ play a key role in the gradient descent step by adjusting its step size adaptively. For simplicity, the parameter α is fixed and treated as a hyper parameter.

As described in the last section, the parameters $\{\gamma_t\}_{t=1}^T$ are optimized by the standard mini-batch training. The ith training data $d^i \triangleq (x^i, y^i)$ is generated randomly, i.e., $x^i \in \{-1, +1\}^n$ is generated uniformly at random and the corresponding y^i is then generated according to $y^i = Ax^i + w$ with a given A. A mini-batch consists of D training data $\mathcal{D} \triangleq \{d^1, d^2, \ldots, d^D\}$. In the following experiment, a matrix A is randomly generated for each mini-batch. Each element of A follows the Gaussian PDF with mean 0 and variance 1.

For each round of a training process, we feed these mini-batches to the TPG algorithm to minimize the squared loss function $L(\Theta_t) \triangleq D^{-1} \sum_{d^i \in \mathcal{D}} \|x^i - \hat{x}^t(y^i)\|_2^2$, where $\hat{x}^t(y) \triangleq s_{t+1}$ is the output of the TPG algorithm with t iterations and $\Theta_t \triangleq \{\gamma_1, \ldots, \gamma_t\}$ is a set of trainable parameters up to the tth round. A back propagation process evaluates the gradient $\nabla L(\Theta_t)$ and it is used for updating the set of parameters as $\Theta_t := \Theta_t + \Delta$ where Δ is determined by a SGD type algorithm such as the Adam optimizer.

It should be remarked that a simple shingle-shot training for a whole process by letting $t = T$ does not work well (see also Fig. 2) because the vanishing gradient phenomenon prevents appropriate parameter updates due to the fact that the derivative of the soft projection function (5) becomes nearly zero almost everywhere. In order to avoid the vanishing gradient phenomenon, we use an alternative approach, i.e., *incremental training* as TISTA [14]. In the incremental training, the parameters $\{\gamma_t\}_{t=1}^T$ are sequentially trained from Θ_1 to Θ_T in an incremental manner. The details of the incremental training is as follows. At first, Θ_1 is trained by minimizing $L(\Theta_1)$. After finishing the training of Θ_1, the values of trainable parameters in Θ_1 are copied to the corresponding parameters in Θ_2. In other words, the results of the training for Θ_1 are taken over to Θ_2 as the initial values. For each round of the incremental training which is called a *generation*, K mini-batches are processed.

We show the numerical demonstration of the TPG algorithm. In the experiment, the noise variance is fixed to $\sigma^2 = 4.0$. The number of iterations of the TPG algorithm is $T = 20$. In the training process, we use $K = 100$ mini-batches per generation. The mini-batch size is set to $D = 200$ and Adam optimizer [18] with learning rate 0.0005 is used for the parameter updates. The initial value of the trainable parameters are given by $\gamma_t = 1.0 \times 10^{-4}$ $(t = 1, \ldots, T)$. The softness parameter is fixed to $\alpha = 8.5$ for the TPG algorithm.

Figure 2 shows the mean squared error (MSE) as a function of iteration steps of the plain PG algorithm based on (2),
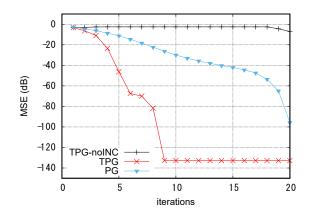

Fig. 2. MSE as a function of iteration steps. The curve (PG) represents the MSE of the plain PG algorithm with $\gamma = 6.5 \times 10^{-4}$. The curve (TPG) corresponds to the MSE of the TPG algorithm and the curve (TPG-noINC) corresponds to the TPG algorithm without incremental training.

(3) $(\alpha = 6.0, \gamma = 6.5 \times 10^{-4})$ and the TPG algorithms based on (4), (5) (with/without incremental training). The MSE is defined by $10 \log_{10}(E[\|x - \hat{x}^t(y)\|_2^2]/n)$ (dB) and it is estimated from 10^4 random samples of A, y and x. The parameter $\gamma = 6.5 \times 10^{-4}$ in the plain PG algorithm is the optimal value for $T = 20$ (See also Fig.3). From Fig. 2, we can observe that the TPG algorithm provides much smaller MSEs than those of the plain PG algorithm. The MSE of TPG achieves -80 dB at $t = 8$ but the PG yields the smaller MSE after $t = 19$. Namely, TPG shows much faster convergence and it implies that the optimal parameter tuning drastically improves the convergence speed. This is an example of the data-driven acceleration of convergence. The effect of the incremental training can be confirmed by comparing the MSEs of the TPG algorithms with/without incremental training. The MSE curve of TPG-noINC is almost flat, indicating that the parameter tuning is not successful in the case of the TPG algorithm without incremental training.

In Fig. 3, we show the γ dependence of the MSE performance in the plain PG algorithm. We find that the parameter γ must be selected carefully to obtain appropriate convergence. In other words, the sweet spot of γ is relatively narrow, i.e., close neighborhood of 6×10^{-4} is only allowable choice for achieving -100 dB at $T = 200$. This means that optimization of the step size is critical even for the plain PG algorithm. In addition, the TPG algorithm achieves the lower MSE performance (around -130 dB) which cannot be achieved by the plain PG algorithm. This fact implies that having independent step size parameters for each iteration provides substantial improvement on the quality of the solution.

IV. PROBLEM SETTING FOR OVERLOADED MIMO CHANNELS

The section describes the channel model and introduces several definitions and notation. The numbers of transmit and receive antennas are denoted by n and m, respectively. We only consider the overloaded MIMO scenario in this paper where $m < n$ holds. It is also assumed that the transmitter
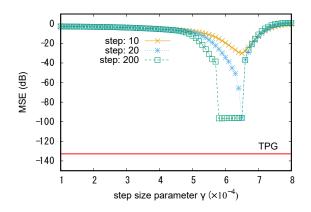
Fig. 3. γ dependence of the MSE performance in the plain PG algorithm. The horizontal solid line represents the MSE of TPG with $T = 20$.

Fig. 4. The tth layer of the TPG-detector. The trainable parameters are γ_t and θ_t.

does not use precoding and that the receiver perfectly knows the channel state information, i.e., the channel matrix.

Let $\tilde{x} \triangleq [\tilde{x}_1, \tilde{x}_2, \ldots, \tilde{x}_n]^T \in \tilde{\mathbb{S}}^n$ be a vector which consists of a transmitted symbol $\tilde{x}_j$ ($j = 1, \ldots, n$) from the jth antenna. The symbol $\tilde{\mathbb{S}} \subset \mathbb{C}$ represents a symbol alphabet, i.e., a signal constellation. Similarly, $\tilde{y} \triangleq [\tilde{y}_1, \tilde{y}_2, \ldots, \tilde{y}_m]^T \in \mathbb{C}^m$ denotes a vector composed of a received symbol $\tilde{y}_i$ ($i = 1, \ldots, m$) by the ith antenna. A flat Rayleigh fading channel is assumed here and the received symbols $\tilde{y}$ then reads $\tilde{y} = \tilde{H}\tilde{x} + \tilde{w}$, where $\tilde{w} \in \mathbb{C}^m$ consists of complex Gaussian random variables with zero mean and covariance $\sigma_w^2 I$. The matrix $\tilde{H} \in \mathbb{C}^{m \times n}$ is a channel matrix whose (i, j) entry $\tilde{h}_{i,j}$ represents a path gain from the jth transmit antenna to the ith receive antenna. Each entry of $\tilde{H}$ independently follows the complex Gaussian distribution with zero mean and unit variance. For the following discussion, it is convenient to derive an equivalent channel model defined over $\mathbb{R}$, i.e., $y = Hx + w$, where

$$
y \triangleq \begin{bmatrix} \mathrm{Re}(\tilde{y}) \\ \mathrm{Im}(\tilde{y}) \end{bmatrix} \in \mathbb{R}^M, \ H \triangleq \begin{bmatrix} \mathrm{Re}(\tilde{H}) & -\mathrm{Im}(\tilde{H}) \\ \mathrm{Im}(\tilde{H}) & \mathrm{Re}(\tilde{H}) \end{bmatrix},
$$

$$
x \triangleq \begin{bmatrix} \mathrm{Re}(\tilde{x}) \\ \mathrm{Im}(\tilde{x}) \end{bmatrix} \in \mathbb{S}^N, \ w \triangleq \begin{bmatrix} \mathrm{Re}(\tilde{w}) \\ \mathrm{Im}(\tilde{w}) \end{bmatrix} \in \mathbb{R}^M,
$$

and $(N, M) \triangleq (2n, 2m)$. The signal set $\mathbb{S}$ is the real counter part of $\tilde{\mathbb{S}}$. The matrix $H \in \mathbb{R}^{M \times N}$ is converted from $\tilde{H}$. Similarly, the noise vector w consists of i.i.d. random variables following the Gaussian distribution with zero mean and variance $\sigma_w^2/2$. Signal-to-noise ratio (SNR) per receive antenna is then represented by SNR $\triangleq E_s/N_0 = N/\sigma_w^2$, where $E_s \triangleq \mathbb{E}[\|\tilde{H}\tilde{x}\|_2^2]/m$ stands for the signal power per receive antenna and $N_0 \triangleq \sigma_w^2$ stands for the noise power per receive antenna. Throughout the paper, we assume the QPSK modulation format, i.e., $\tilde{\mathbb{S}} \triangleq \{1 + j, -1 + j, -1 - j, 1 - j\}$, which is equivalent to the BPSK modulation $\mathbb{S} \triangleq \{-1, +1\}$.

V. TRAINABLE PROJECTED GRADIENT (TPG)-DETECTOR

The maximum likelihood estimation rule for the MIMO channel defined above is given by

$$
\hat{x} = \mathrm{argmin}_{x \in \{-1, +1\}^N} \|Hx - y\|_2^2. \tag{6}
$$
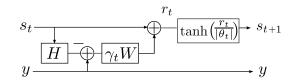
This problem is a non-convex problem and finding the global minimum is computationally intractable for a large scale problem. Our proposal, TPG-detector, is based on the projected gradient method for solving the above non-convex problem approximately. The process of TPG-detector is described by the following recursive formulas:

$$
r_t = s_t + \gamma_t W(y - Hs_t), \tag{7}
$$

$$
s_{t+1} = \tanh\left(\frac{r_t}{|\theta_t|}\right), \tag{8}
$$

where $t (= 1, \ldots, T)$ represents the index of an iterative step (or layer) and we set $s_1 = 0$ as the initial value. This algorithm estimates a transmitted signal x from the received signal y and outputs the estimate $\hat{x} = s_{T+1}$ after T iterative steps.

The steps (7) and (8) correspond to the gradient descent step and to the projection step, respectively, as described in Section IIIs. The matrix W in the gradient step (7) is the Moore-Penrose pseudo inverse matrix of H, i.e., $W \triangleq H^T(HH^T)^{-1}$. Precisely speaking, W should be H^T as in (4). However, we adopt the modification inspired by [19] because this modification improves the BER performance of the proposed scheme. As in the case in (5), we use the hyperbolic tangent function as the soft projection.

The trainable parameters of TPG-detector are $2T$ real scalar variables $\{\gamma_t\}_{t=1}^T$ and $\{\theta_t\}_{t=1}^T$ in (7) and (8), respectively. The parameters $\{\gamma_t\}_{t=1}^T$ in the gradient step control the step size of a move of the search point. In order to achieve fast convergence, appropriate setting of these step size parameters is of critical importance as described in Section III. It should be remarked that similar constant trainable parameters are also introduced in the structure of TISTA [14]. The parameters $\{\theta_t\}_{t=1}^T$ control the softness of the soft projection in (8). One of the advantages of TPG-detector is that the number of trainable parameters is small, i.e., $O(T)$, and it leads to fast and stable training processes. For example, the number of trainable parameters of TPG-detector is constant to N and M though a DMD [15] contains $O(N^2T)$ parameters in T layers.

The computational complexity of TPG-detector per iteration is $O(MN)$ because one needs to calculate the vector-matrix products Hs_t and $W(y - Hs_t)$ that take $O(MN)$ computational steps. We need to calculate the pseudo inverse matrix W taking $O(M^3)$ computational steps only when H changes.

The TPG-detector is trained based on the incremental training described in Section III. The training data is generated randomly according to the channel model with fixed variance σ_w^2 corresponding to a given SNR. As described in Section IV,

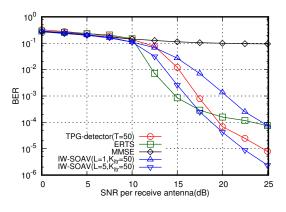Fig. 5. BER performance for $(N, M) = (200, 128)$.

Fig. 6. BER performance for $(N, M) = (300, 192)$.

we assume a practical situation in which a channel matrix H is a random variable. According to this assumption, a matrix H is randomly generated for each mini-batch in a training process of TPG-detector.

VI. NUMERICAL RESULTS

In this section, we show the detection performance of TPG-detector and compare it to that of known algorithms such as IW-SOAV which is known as one of the most efficient iterative algorithms for massive overloaded MIMO systems.

A. Experimental setup

A transmitted vector x is generated uniformly at random. The BER is then evaluated for a given SNR. We use randomly generated channel matrices for BER estimation.

TPG-detector was implemented by PyTorch 0.4.0 [20]. The following numerical experiments were carried out on a PC with GPU NVIDIA GerForce GTX 1080 and Intel Core i7-6700K CPU 4.0GHz × 8. In this paper, a training process is executed with $T = 50$ rounds using the Adam optimizer [18]. A training process takes within 25 minutes under our environment. To calculate the BER of TPG-detector, a sign function $\mathrm{sgn}(z)$ which takes -1 if $z \leq 0$ and 1 otherwise is applied to the final estimate s_{T+1}.

As the baselines of detection performance, we use the ERTS [4], IW-SOAV [6], and the standard MMSE detector. The ERTS is a heuristic algorithm based on a tabu search for overloaded MIMO systems. The parameters of ERTS is based on [4]. The IW-SOAV is a double loop algorithm whose inner loop is the W-SOAV optimization recovering a signal using a proximal operator. Each round of the W-SOAV takes $O(MN)$ computational steps, which is comparable to that of TPG-detector. After finishing an execution of the inner loop with K_{itr} iterations, several parameters are then updated in a re-weighting process based on a tentative recovered signal. This procedure is repeated L times in the outer loop. The total number of steps of the IW-SOAV is thus $K_{\mathrm{itr}}L$. In the following, we use the simulation results in [6] with $K_{\mathrm{itr}} = 50$.
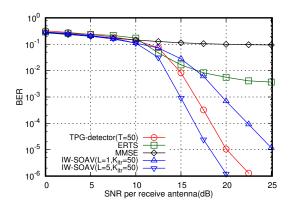
B. Main results

We first present the BER performance of each detector as a function of SNR for $(N, M) = (200, 128)$ in Fig. 5. The results show that the MMSE detector fails to detect transmitted signals reliably (BER $\simeq 10^{-1}$) because the system is underdetermined. The ERTS detector shows the best BER performance in a middle SNR region where SNR is between 10 dB and 20 dB. On the other hand, TPG-detector exhibits the BER performance superior to that of the IW-SOAV ($L = 1$), i.e., TPG-detector achieves approximately 5 dB gain at BER $= 10^{-4}$ over the IW-SOAV ($L = 1$). Note that the computational cost for executing TPG-detector with $T = 50$ is almost comparable to that of the IW-SOAV ($L = 1$). More interestingly, the BER performance of TPG-detector is fairly close to that of IW-SOAV ($L = 5$). For example, with SNR $= 20$ dB, the BER estimate of TPG-detector is 6.8×10^{-5} whereas that of the IW-SOAV ($L = 5$) is 4.3×10^{-5}. It should be noted that the total number iterations of the IW-SOAV ($L = 5$) is 250.

Figure 6 shows the BER performance for $(N, M) = (300, 196)$. In this case, ERTS shows relatively poor BER performance without a narrow region. TPG-detector successfully recovers transmitted signals with lower BER than that of the IW-SOAV($L = 1$). It again achieves about 5 dB gain against the IW-SOAV($L = 1$) at BER $= 10^{-5}$. Although the IW-SOAV ($L = 5$) shows considerable performance improvements in this case, the gaps between the curves of TPG-detector and the IW-SOAV ($L = 5$) are about 2 dB at BER $= 10^{-5}$.

In Fig. 7, we show the BER performance of TPG-detector and IW-SOAV ($L = 1$) for some antenna sizes N with the rate $M/N = 0.6$ fixed. The gap of their BER performances is especially large for SNR$= 20$ (dB). We also find that the gain of the TPG-detector increases as N grows though these algorithms have the same computational costs. It is confirmed that the TPG-detector outperforms other low-complexity algorithms especially in the massive overloaded MIMO channels.

Finally, Fig. 8 displays the learned parameters $\{\gamma_t, |\theta_t|\}$ of TPG-detector after a training process as a function of a layer index $t(= 1, \ldots, T)$. We find that they exhibit a zigzag shape with damping amplitude similar to that observed
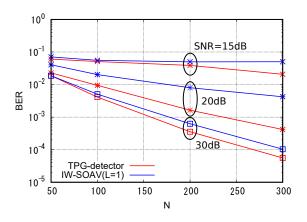
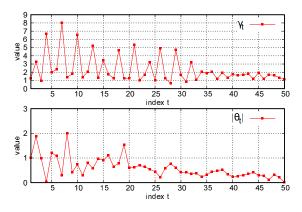Fig. 7. Antenna size dependency of BER performance for fixed rate $M/N = 0.6$.

Fig. 8. Sequences of learned parameters γ_t (upper) and $|\theta_t|$ (lower); $(N, M) = (300, 192)$, SNR = 20 (dB), $1 \le t \le T = 50$.

in TISTA [14]. The parameter γ_t, the step size of a linear estimator, is expected to accelerate the convergence of the signal recovery. Theoretical treatments for providing reasonable interpretation on these characteristic shapes of the learned parameters are interesting open problems.

VII. CONCLUDING REMARKS

In this paper, we proposed TPG-detector, a deep learning-aided iterative decoder for massive overloaded MIMO channels. TPG-detector contains two trainable parameters for each layer: γ_t controlling a step size of the linear estimator and θ_t dominating strength of the nonlinear estimator. The total number of the trainable parameters in T layers is thus $2T$, which is significantly smaller than that used in the previous studies such as [15], [16]. This fact promotes fast and stable training processes for TPG-detector. The numerical simulations show that TPG-detector outperforms the state-of-the-art IW-SOAV ($L = 1$) by a large margin and achieves a comparable detection performance to the IW-SOAV ($L = 5$). TPG-detector therefore can be seen as a promising iterative detector for overloaded MIMO channels providing an excellent balance between a low computational cost and a reasonable detection performance. There are several open problems regarding this study. First, adding a re-weighting process similar to the one used in the

IW-SOAV ($L \ge 2$) to TPG-detector seems an interesting direction to improve the detection performance. Secondly, enhancing TPG-detector toward a large constellation such as QAM is a practically important problem.

REFERENCES

[1] S. Yang and L. Hanzo, "Fifty years of MIMO detection: the road to large-scale MIMOs," IEEE Comm. Surveys and Tutorials, vol. 17, no. 4, pp. 1941-1988, Fourthquarter 2015.
[2] D. A. Shnidman, "A generalized Nyquist criterion and an optimum linear receiver for a pulse modulation system," The Bell System Technical Journal, vol. 46, no. 9, pp. 2163-2177, Nov. 1967.
[3] K. K. Wong, A. Paulraj, and R. D. Murch, "Efficient high-performance decoding for overloaded MIMO antenna systems," IEEE Trans. Wireless Commun., vol. 6, no. 5, pp. 1833-1843, May 2007.
[4] T. Datta, N. Srinidhi, A. Chockalingam, and B. S. Rajan, "Low-complexity near-optimal signal detection in underdetermined large-MIMO systems," in Proc. National Conf. Comm., Feb. 2012, pp. 1-5.
[5] Y. Fadlallah, A. Aïssa-El-Bey, K. Amis, D. Pastor, and R. Pyndiah, "New decoding strategy for underdetermined MIMO transmission using sparse decomposition," in Proc. in Proc. 2013 21st Eur. Signal Proc. Conf., Sep. 2013, pp. 1-5.
[6] R. Hayakawa and K. Hayashi, "Convex optimization-based signal detection for massive overloaded MIMO systems," in IEEE Trans. Wireless Comm., vol. 16, no. 11, pp. 7080-7091, Nov. 2017.
[7] R. Hayakawa, K. Hayashi, H. Sasahara, and M. Nagahara, "Massive overloaded MIMO signal detection via convex optimization with proximal splitting," in Proc. 2016 24th Eur. Signal Proc. Conf., Aug./Sep. 2016, pp. 1383-1387.
[8] M. Nagahara, "Discrete signal reconstruction by sum of absolute values" IEEE Signal Process. Lett., vol. 22, no. 10, pp. 1575–1579, Oct. 2015.
[9] G. E. Hinton and R. R. Salakhutdinov, "Reducing the dimensionality of data with neural networks," Science, vol. 313, no. 5786, pp. 504-507, Jun. 2006:
[10] B. Aazhang, B. P. Paris, and G. C. Orsak, "Neural networks for multiuser detection in code-division multiple-access communications," IEEE Trans. Comm., vol. 40, no. 7, pp. 1212-1222, Jul. 1992.
[11] E. Nachmani, Y. Beéry, and D. Burshtein, "Learning to decode linear codes using deep learning," *2016 54th Annual Allerton Conf. Comm., Control, and Computing*, 2016, pp. 341-346.
[12] K. Gregor and Y. LeCun, "Learning fast approximations of sparse coding," in Proc. 27th Int. Conf. Machine Learning, pp. 399–406, 2010.
[13] I. Daubechies, M. Defrise, and C. De Mol, "An iterative thresholding algorithm for linear inverse problems with a sparsity constraint," Comm. Pure and Appl. Math., vol. 57, no. 11, pp. 1413-1457, Aug. 2004.
[14] D. Ito, S. Takabe, and T. Wadayama, "Trainable ISTA for sparse signal recovery," IEEE Int. Conf. Comm., Workshop on Promises and Challenges of Machine Learning in Communication Networks, Kansas city, May. 2018. (arXiv:1801.01978)
[15] N. Samuel, T. Diskin, and A. Wiesel, "Deep MIMO detection," *2017 IEEE 18th Int. Workshop Signal Processing Advances in Wireless Comm.*, Jul. 2017, pp. 1-5.
[16] N. Samuel, T. Diskin, and A. Wiesel, "Learning to detect," arXiv: 1805.07631, 2018.
[17] D. Divsalar, M. K. Simon, and D. Raphaeli, "Improved parallel interference cancellation for CDMA", IEEE Trans. Commun., vol. 46, no. 2, pp. 258-268, Feb. 1998.
[18] D. P. Kingma and J. L. Ba, "Adam: A method for stochastic optimization," arXiv:1412.6980, 2014.
[19] J. Ma and L. Ping, "Orthogonal AMP," IEEE Access, vol. 5, pp. 2020-2033, Jan. 2017.
[20] PyTorch, https://pytorch.org